

Structural Study of Amorphous Tellurium(II) Halides $\text{TeCl}_{2-x}\text{I}_x$ ($x = 0.5, 0.1$): X-ray Diffraction and Reverse Monte Carlo Simulations

Nikolay Zotov,^{*,†} Johannes Beck,[‡] Bärbel Knopp,[‡] and Armin Kirfel[§]

Forschungszentrum CAESAR, Ludwig-Erhard-Allee 2, D-53175 Bonn, Germany, Institut für Anorganische Chemie, Universität Bonn, Gerhard-Domagk-Strasse 1, D-53121 Bonn, Germany, and Mineralogisch-Petrologisches Institut, Universität Bonn, Poppelsdorfer Schloss, D-53115 Bonn, Germany

Received December 4, 2006

The addition of small amounts of iodine to thermodynamically instable TeCl_2 yields amorphous, glassy tellurium(II) halides $\text{TeCl}_{2-x}\text{I}_x$ ($0.1 < x < 0.5$), which were prepared by rapid quenching of melts with the respective compositions. At ambient temperature, these glassy solids are sufficiently stable to be handled and investigated by analytical methods. High-energy X-ray diffraction and reverse Monte Carlo simulations of two compositions $\text{TeCl}_{2-x}\text{I}_x$, $x = 0.1$ and 0.5 , show that these glasses are made up of structural fragments that are present in both tellurium tetrahalides and in low-valent tellurium subhalides. In both glasses, the Te–Te bonding shows narrow coordination distribution with a mean total coordination number for the Te atoms of 4.1 ± 1.3 and a mean Te–Te coordination number of 0.7 ± 0.7 . Accordingly, the mean Cl–Te coordination number is 1.7 ± 0.8 and the mean I–Te coordination number is 1.6 ± 0.7 . The medium-range order increases with increasing iodine content.

Introduction

Tellurium forms halides in various oxidation states, ranging from +VI in hexafluoride down to oxidation states below +I in the subhalides. A typical feature of the low-valent compounds is the occurrence of Te–Te bonds. Besides metastable phases like Te_2Cl , low-valent halides like Te_3Cl_2 or Te_2Br are known to be thermodynamically stable. A particularly large structural diversity is found for the tellurium subiodides.^{1–3}

The tellurium halides with oxidation state +II present a special group of compounds. They are well-known as gas-phase species and have been studied intensively. Vibrational spectroscopy⁴ and electron diffraction⁵ of TeCl_2 gas have shown the structure to be made up of bent molecules with a Te–Cl bond length of 2.33 Å and a Cl–Te–Cl angle of about 97°. Tellurium tetrahalides, which are stable at ambient

temperature, decompose at elevated temperatures according to $\text{TeX}_4 \rightarrow \text{TeX}_2 + \text{X}_2$ ($\text{X} = \text{Cl}, \text{Br}, \text{I}$). Vapor pressure measurements have shown that above 500 °C the partial pressure of TeCl_4 in a closed system is less than 0.5% of the total pressure and TeCl_2 is the dominant species.⁶ The phase diagrams of the solid and liquid phases of the two-component systems Te/Cl, Te/Br, and Te/I do not show the existence of condensed phases of the composition TeX_2 .⁷ Under ambient conditions TeI_2 is an endothermic compound with an enthalpy of formation of $\Delta H^f = +80 \text{ kJ mol}^{-1}$.⁸ Despite of the fact that the synthesis of solid TeCl_2 has been described in the literature,^{9–10} its existence was denied several times.^{11–13} Straightforward synthesis of tellurium dihalides is achieved by the reduction of the respective tetrahalides with elemental Te according to the reaction $\text{TeX}_4 + \text{Te} \rightarrow 2\text{TeX}_2$. Any thermal treatment like slow cooling or holding the temperature close to the melting points of TeX_2 (which

* To whom correspondence should be addressed. E-mail: zotov@caesar.de.

† Forschungszentrum CAESAR.

‡ Institut für Anorganische Chemie, Universität Bonn.

§ Mineralogisch-Petrologisches Institut, Universität Bonn.

- (1) Kniep, R.; Mootz, D.; Rabenau, A. *Angew. Chem.* **1973**, *85*, 504.
- (2) Kniep, R.; Mootz, D.; Rabenau, A. *Z. Anorg. Allg. Chem.* **1976**, *422*, 17.
- (3) Kniep, R.; Beister, H.-J. *Angew. Chem.* **1985**, *97*, 399.
- (4) Kovács, A.; Konings, R. J. M. *J. Mol. Struct.* **1997**, *410–411*, 407.
- (5) Fernholt, L.; Haaland, A.; Volden, H. V.; Kniep, R. *J. Mol. Struct.* **1985**, *128*, 29.

- (6) Oppermann, H. *Z. Anorg. Allg. Chem.* **1977**, *434*, 239.
- (7) Rabenau, A.; Rau, H. *Z. Anorg. Allg. Chem.* **1973**, *395*, 273.
- (8) Oppermann, H.; Stöver, G.; Wolf, E. *Z. Anorg. Allg. Chem.* **1976**, *419*, 200.
- (9) Lindner, K.; Apolant, L. *Z. Anorg. Allg. Chem.* **1924**, *136*, 381.
- (10) Aynsley, E. E. *J. Chem. Soc.* **1953**, 3016.
- (11) Damiens, A. *Ann. Chim. Phys.* **1923**, *9*, 44.
- (12) Voigt, A.; Biltz, W. *Z. Anorg. Allg. Chem.* **1924**, *133*, 277.
- (13) Christensen, G. C.; Alstad, J. *Radiochem. Radioanal. Lett.* **1973**, *13*, 227.

are about 200 °C⁷) has to be avoided because decomposition into a tetrahalide and elemental Te or a subhalide will occur. We have attempted to obtain TeCl_2 as a metastable solid by rapid quenching from the gas phase but in the end without success (details are given in the Experimental Section).

Te-rich halides are known to form glassy solids. Tellurium subiodide bromide $\text{Te}_2\text{Br}_{1-x}\text{I}_x$ ($x \leq 0.75$) can be obtained in the glassy state by quenching a melt of the respective composition. Photoelectron spectroscopy and X-ray diffraction have shown that the structure possesses a short-range order (SRO) analogous to that in the crystalline phases Te_2Br and Te_2I .¹⁴ Studies on glasses of these compositions have recently been repeated using atomic force microscopy¹⁵ and diffraction of hard X-rays as well as neutrons¹⁶ resulting in more detailed structure models. The medium-range structure in glasses of the composition Te_3X_2 ($X = \text{Cl}, \text{Br}$) was explored by ¹²⁵Te absorption and ¹²⁹I emission Mössbauer spectroscopy. Again, a structure model similar to the chainlike structure of crystalline Te_3Cl_2 was derived from the spectroscopic data.¹⁷ The easy glass formation for compositions with halogen/tellurium ratios $X/\text{Te} < 0.667$ is probably due to the fact that Te itself is an easy glass former.¹⁸

So far, there is no information available for the structure on the atomic scale of solid crystalline Te(II) halides, TeX_2 , mainly due to their thermodynamical instability. The disproportionation reaction $2\text{TeX}_2 \rightarrow \text{TeX}_4 + \text{Te}$ is already at ambient temperature so fast that it is impossible to obtain stable samples allowing for spectroscopic or diffraction experiments. We have found, however, that mixing Cl and I has a large stabilizing effect for a wide range of compositions. Thus, we were able to synthesize glassy Te(II) halides with compositions $\text{TeCl}_{2-x}\text{I}_x$ that are stable enough to be investigated by diffraction methods. Since it seems not possible to obtain Te(II) halides in the crystalline state, we attempted to find insights about the structure in the glassy state. The various steps of the preparation and results for the first structure models of solid amorphous Te(II) halides are presented below.

Experimental Section

All preparations were carried in an argon-filled glovebox under oxygen- and water-free atmosphere. The starting materials were checked for purity via X-ray powder diffraction. Additional reflections indicating impurities were not detected. Elemental tellurium was sublimated twice at 750 °C using a dynamic vacuum in quartz tubes. TeCl_4 was prepared by passing a stream of dry Cl_2 over Te at 350 °C and final sublimation in vacuum. Iodine was thoroughly mixed with P_4O_{10} and heated in vacuum to 50 °C. Sublimating I_2 was then collected on a cold finger.

(14) Shevchik, N. J.; Kniep, R. *J. Chem Phys.* **1974**, *60*, 3011.

(15) Kayser, T.; Ostadrahim, A. H.; Schlenz, H.; Beck, J.; Wandelt, K. *J. Non-Cryst. Solids* **2005**, *351*, 1097.

(16) Zotov, N.; Schlenz, H.; Beck, J.; Knopp, B.; Schäfer, W.; Kirfel, A.; Javari, P. *J. Non-Cryst. Solids* **2005**, *351*, 3095.

(17) Wells, J.; Bresser, W. J.; Boolchand, P.; Lucas, J. *J. Non-Cryst. Solids* **1996**, *195*, 170.

(18) Borisova, Z. V. *Glassy Semiconductors*; Plenum Press: New York, 1981.

Attempted Preparation of TeCl_2 by Rapid Quenching of TeCl_2 Gas in a Closed System. A 48 mg amount of Te and 102 mg of TeCl_4 were filled into a quartz capsule of 15 cm length and 0.8 cm internal diameter. After evacuation and flame-sealing, a thick platinum wire was wound around the ampule to facilitate fast immersion into the quenching liquid. The capsule was then heated for 1 h at 500 °C in an horizontal tube furnace. The internal pressure was estimated to be 10 bar. When visual inspection in the hot state showed no remaining solid material in the ampule (suggesting total conversion of the solid material into TeCl_2 vapor), the hot ampule was dropped directly into an ice/water bath upon which the gas phase precipitated completely as a dark layer. The mass/cm² of this layer was weighed to be about 4 mg, which conforms with the amount of 150 mg of “ TeCl_2 ” starting material and the inner surface of the ampule (about 37 cm²). Thus, all of the starting Te and TeCl_4 had deposited on the wall of the reaction vessel. The subsequent inspection of the deposited material by powder diffractometry with Cu K α radiation seemed initially promising since no reflection lines were found. After several hours, however, the sample showed Bragg reflections which could unambiguously be assigned to trigonal tellurium and monoclinic TeCl_4 .¹⁹

Attempted Preparation of TeCl_2 by Rapid Quenching of a TeCl_2 Gas Flow. A melt of the composition TeCl_2 was prepared from equimolar amounts of Te and TeCl_4 . In a closed glass apparatus, a stream of dry argon was flushed with about 100 mL/min over the black melt held at 400 °C. When a cold finger cooled with dry ice to -70 °C was placed in the gas flow at a distance of 5 cm, a black material started to deposit on it. After 6 h the deposited material was scratched from the cold finger and analyzed by X-ray diffraction. The powder diffractograms of samples performed under slightly different conditions always contained reflections of TeCl_4 .

Preparation of Amorphous $\text{TeCl}_{2-x}\text{I}_x$. For the preparation of amorphous $\text{TeCl}_{2-x}\text{I}_x$ we used specially designed glass ampules which allow both equilibration of the melt (by stirring) and rapid quenching within one and the same closed apparatus. The glass ampules had the form of a pear with a long thin-walled end (Figure 1a). The overall length was 12 cm, and the diameter of the capillary was 0.2 cm. After being filled with the respective amounts of Te, TeCl_4 , and I_2 , evacuated, and flame-sealed, the ampule was connected to an electric motor and rotated slowly (15–20 rotations/min) in a cylindrical oven inclined at 45° as shown in Figure 1b. After 20 h of constant rotation at 300 °C the whole assembly was put into downward position (Figure 1c), the rotation was stopped, and the melt was allowed to settle in the thin end of the ampule. After 3 min the ampule was disconnected from the motor and immediately dropped into a bath of liquid mercury cooled to a temperature of -30 °C (Figure 1d).

Density Determination. The densities at 25 °C of two samples with the compositions $\text{TeCl}_{1.9}\text{I}_{0.1}$ and $\text{TeCl}_{1.5}\text{I}_{0.5}$ were determined pycnometrically using dodecane as sealing liquid. Two measurements for each composition on samples from different batches yielded 3.59(10) and 3.53(8) g cm⁻³ for $\text{TeCl}_{1.9}\text{I}_{0.1}$ and 4.08(15) and 3.79(5) g cm⁻³ for $\text{TeCl}_{1.5}\text{I}_{0.5}$.

Thermal Analyses. Samples of both compositions $\text{TeCl}_{1.9}\text{I}_{0.1}$ and $\text{TeCl}_{1.5}\text{I}_{0.5}$ were investigated by differential scanning calorimetry using a Netzsch calorimeter DSC 204 F1 and closed Al containers as well as by differential thermal analysis/thermogravimetry using a Netzsch DTA/TG STA 429 instrument and open corundum crucibles.

(19) Buss, B.; Krebs, B. *Inorg. Chem.* **1971**, *10*, 2795.

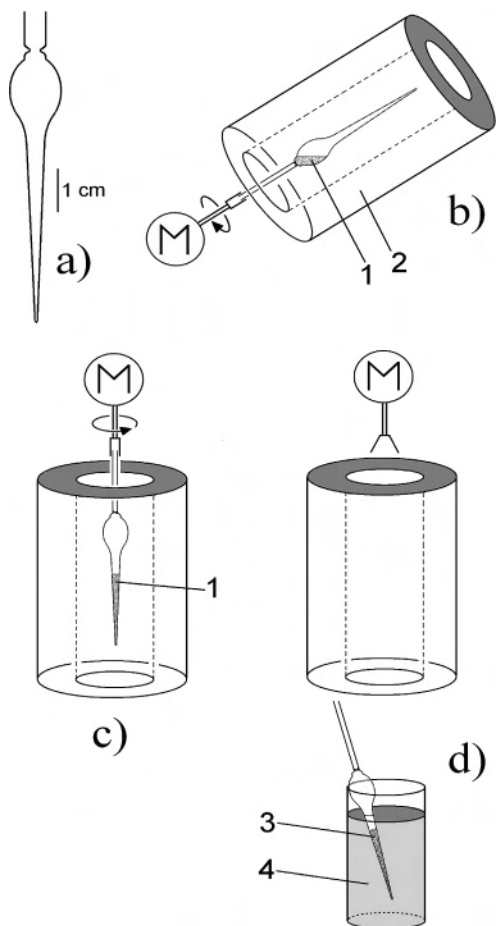


Figure 1. Apparatus for the synthesis of amorphous low valent Te halides: (a) special glass ampule before filling; (b) position of the ampule during equilibration; (c) position of the ampule after quenching; (d) position of the ampule after quenching. Legend: M = electric motor with adjustable speed; 1 = $\text{TeCl}_{2-x}\text{I}_x$ melt; 2 = tube oven; 3 = solidified, glassy $\text{TeCl}_{2-x}\text{I}_x$; 4 = liquid mercury at -30°C .

X-ray Diffraction. High-energy X-ray diffraction data ($E = 138.4\text{ keV}$) for two glass samples, $\text{TeCl}_{1.9}\text{I}_{0.1}$ and $\text{TeCl}_{1.5}\text{I}_{0.5}$, were collected at the wiggler synchrotron beamline BW5 at HASYLAB/DESY (Hamburg, Germany). This instrument operates with a Si(111) Laue single-crystal incident-beam monochromator and a Ge solid-state detector. Hard X-ray radiation allows a high resolution in real space, as desired for amorphous materials. The experiments were carried out in Debye–Scherrer geometry. The sample holder was a pure silica glass capillary of 0.001 cm wall thickness and 0.1 cm diameter. The capillaries were placed in a vacuum chamber (pressure $\sim 1.3 \times 10^{-3}\text{ bar}$) to reduce air scattering at low values of Q [$Q = 4\pi \sin(\theta)/\lambda$, where 2θ is the diffraction angle and λ the wavelength used (0.08986 \AA)]. The data were recorded in two ranges: $0.8^\circ < 2\theta < 10.0^\circ$ with steps $\Delta 2\theta = 0.05^\circ$; $9.0^\circ < 2\theta < 27.0^\circ$ with steps $\Delta 2\theta = 0.15^\circ$. The acquisition times were 5 and 20 s for the first and second range, respectively. In both ranges each sample was measured four times for minimizing the influence of beam fluctuations and drifts. The effective absorption coefficients $\mu(E)$ were determined by sample transmission experiments, 1.74 and 2.35 cm^{-1} for $\text{TeCl}_{1.9}\text{I}_{0.1}$ and $\text{TeCl}_{1.5}\text{I}_{0.5}$, respectively. Each data set was first corrected for the decay of the ring current using the primary-beam monitor data, and good internal agreement (variations $\pm 2\%$) was obtained between the corresponding 2θ points of the different runs. The four measurements for each range were then

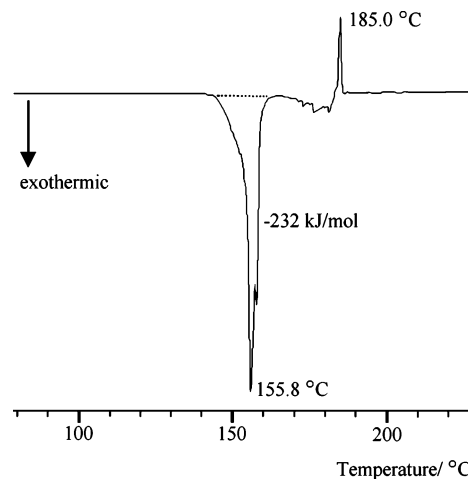


Figure 2. Thermal effects on heating $\text{TeCl}_{1.9}\text{I}_{0.1}$ measured by differential scanning calorimetry. The sample was placed in a closed Al container, and the heating rate was $0.5^\circ\text{C}/\text{min}$.

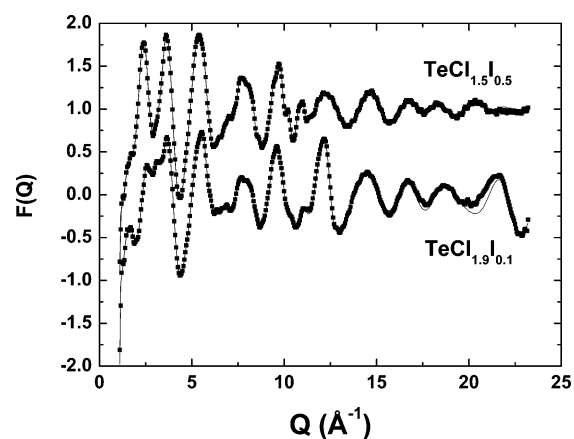


Figure 3. Comparison of the reduced experimental structure factors $F(Q)$ from RMC (thin lines) and experimental X-ray structure factors (squares). For clarity, the data for $\text{Te}_2\text{Cl}_{1.5}\text{I}_{0.5}$ are shifted upward.

averaged, Fourier smoothed, and finally merged into a unique data set for each sample. The subsequent data reduction included corrections for background and empty-capillary scattering (scaled to the sample monitor rate), dead time (approximately $1.3\text{ }\mu\text{s}$), absorption (using the measured μR value and the method of Sabine et al.),²⁰ polarization of the incident beam (horizontal polarization fraction 0.91), inelastic scattering (using the analytical approximation to the incoherent X-ray scattering intensities published in ref 21), and variable sample–detector distance, caused by the linear movement of the detector normal to the primary beam.²² The obtained coherent scattering intensities $F^{\text{coh}}(Q)$ up to $Q_{\text{max}} = 24\text{ \AA}^{-1}$ were normalized to electron units using both the Krogh–Moe²³ and the high-angle²⁴ method. The analytical scattering-factor functions for neutral atoms²⁵ were taken for the calculation of $\langle f^2 \rangle$ and $\langle f \rangle^2$, where $\langle f \rangle = \sum c_i f_i$, $\langle f^2 \rangle = \sum \sum c_i c_j f_i f_j^*$, and c_i and f_i are the atomic concentration and the atomic form factor, respectively, of atom i , the latter corrected for anomalous dispersion.

(20) Sabine, T. M.; Hunter, B. A.; Sabine, W. R.; Ball, C. J. *J. Appl. Crystallogr.* **1998**, *31*, 47.

(21) Balyuzi, H. H. M. *Acta Crystallogr.* **1975**, *A31*, 600.

(22) Poulsen, H. F.; Neufeld, J.; Neumann, H.-B.; Schneider, J. R.; Zeidler, M. D. *J. Non-Cryst. Solids* **1995**, *188*, 63.

(23) Krogh-Moe, J. *Acta Crystallogr.* **1956**, *9*, 951.

(24) Norman, N. *Acta Crystallogr.* **1957**, *10*, 370.

(25) Cromer, D. T.; Mann, J. B. *Acta Crystallogr.* **1968**, *A 24*, 321.

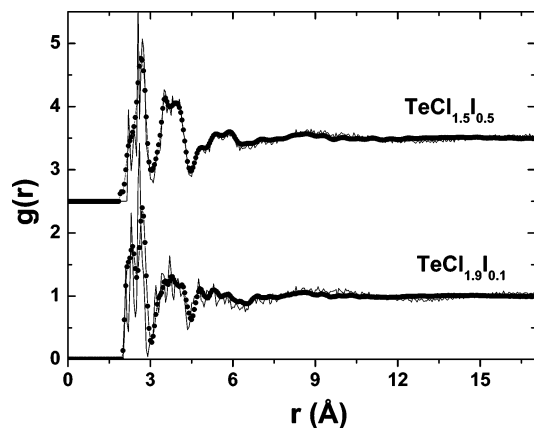


Figure 4. Comparison of the experimental (circles) and RMC (thin lines) total pair correlation functions $g(r)$. For clarity, the data for $\text{Te}_2\text{Cl}_{1.5}\text{I}_{0.5}$ are shifted upward.

RMC Simulations. The reverse Monte Carlo method is a general algorithm²⁶ for developing structural models of disordered materials, consistent with a set of experimental diffraction data and a set of structural constraints. Since the weighting coefficients w_{ij} , $i, j = \text{Te, Cl, and I}$, of the partial structure factors depend on Q in the case of X-ray diffraction, all simulations were done in reciprocal space, using the RMCA²⁷ program. For each composition, simulations were carried out repeatedly with both small (0.3–0.5 Å) and large (5–7.5 Å) maximum allowed random atom moves to obtain best possible fits. Since crystalline phases of TeX_2 are not known (see above), the initial models were constructed by generating random distributions of 2999 atoms with periodic boundary conditions and box edge lengths, 46.04 Å for $\text{TeCl}_{1.9}\text{I}_{0.1}$ and 47.02 Å for $\text{TeCl}_{1.5}\text{I}_{0.5}$, giving the measured bulk glass densities (0.0307 and 0.02885 atoms/Å³, respectively). The minimum-approach distance between all atoms was 1.9 Å in both cases. The number of Te, Cl, and I atoms in the models corresponded to the atomic concentrations. Hard core RMC runs of 3 h duration (RMC simulations without experimental data) were first applied in order to randomly rearrange the atoms in such a way that they fulfill the following distances of minimum approach (cutoff constraints) for the 6 different atom pairs: $R_{\text{Te-Te}}^c = 2.6$ Å, $R_{\text{Te-Cl}}^c = 2.2$ Å, $R_{\text{Te-I}}^c = 2.5$ Å, $R_{\text{Cl-Cl}}^c = 3.2$ Å, $R_{\text{Cl-I}}^c = 3.1$ Å, and $R_{\text{I-I}}^c = 3.8$ Å for $\text{TeCl}_{1.9}\text{I}_{0.1}$ and $R_{\text{Te-Te}}^c = 2.6$ Å, $R_{\text{Te-Cl}}^c = 2.0$ Å, $R_{\text{Te-I}}^c = 2.6$ Å, $R_{\text{Cl-Cl}}^c = 3.2$ Å, $R_{\text{Cl-I}}^c = 3.3$ Å, and $R_{\text{I-I}}^c = 3.8$ Å for $\text{TeCl}_{1.5}\text{I}_{0.5}$. These distances were selected to be some 5–8% smaller than the corresponding minimum distances in crystalline tellurium halides^{1–3} and were slightly readjusted in the subsequent RMC runs. Extensive RMC simulations of $\text{Te}_2\text{Br}_{0.75}\text{I}_{0.25}$ glass have recently shown that the final model structures are not depending on the initial configuration.¹⁶ That is why in this work RMC simulations with different initial configurations were not made.

To prevent overcoordinated atoms, several coordination constraints had to be introduced which served to preclude that the X atoms are coordinated by more than three Te atoms and vice versa that a Te atom is coordinated by more than three other Te atoms, because such local configurations do not exist in any known crystalline tellurium halides. The random initial configurations with the imposed coordination constraints were then used in a series of 12 RMC fits to the total structure factors of duration 137 h for $\text{TeCl}_{1.9}\text{I}_{0.1}$ and 106 h for $\text{TeCl}_{1.5}\text{I}_{0.5}$. For both compositions, convergence was achieved and the imposed coordination constraints

(26) McGreevy, R. L.; Pusztai, L. *Mol. Simul.* **1988**, *1*, 359.

(27) McGreevy, R. L.; Howe, M. A.; Wicks, J. D. *A General Purpose Reverse Monte Carlo Code*, V. 3, 1993.

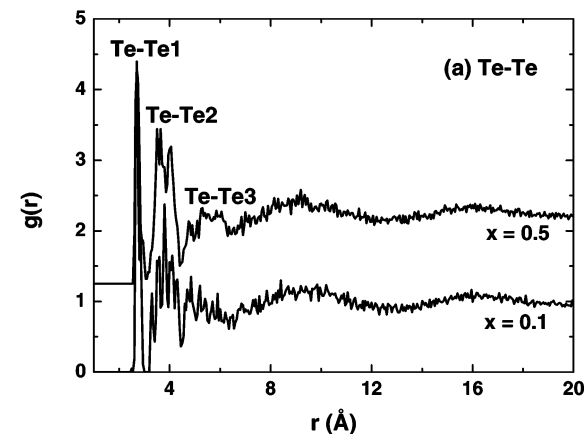
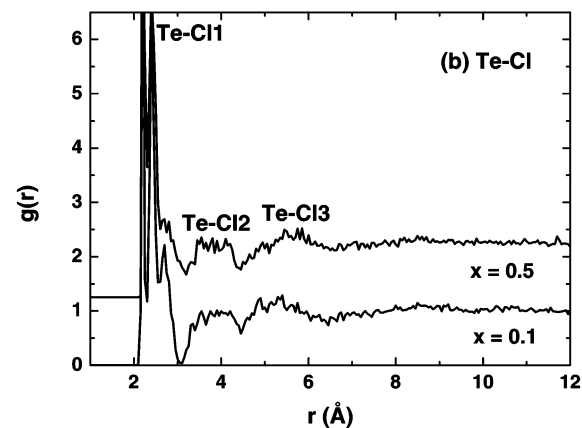
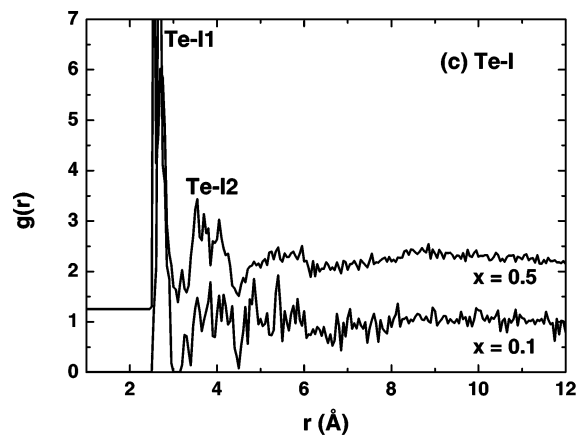


Figure 5. Te–Te, Te–Cl, and Te–I partial pair correlation functions derived from the two RMC models.

were met, with the exception of a few Te atoms (out of 999) which were coordinated by four Te atoms. Also, in the $\text{TeCl}_{1.5}\text{I}_{0.5}$ model, there were several Te–Cl distances smaller than the cutoff distance $R_{\text{Te-Cl}}^c = 2.20$ Å.

Results

Synthesis of Tellurium(II) Halides. All our efforts to synthesize pure crystalline TeCl_2 were unsuccessful. This agrees with the likewise negative results already described in the literature.^{10–12} Even when we used new synthetic procedures like rapid quenching of TeCl_2 vapor, we obtained, in fact, homogeneous amorphous materials, but these samples were unstable and after some hours at ambient temperature Bragg reflections of TeCl_4 showed up in the X-ray powder diffractograms. This thermal instability makes the handling

Table 1. Average and Partial Coordination Numbers (CN) in the Generated Models of TeCl_{2-x}I_x Glasses and Selected Tellurium Halides

CN	RMC models		crystalline phases			
	$x = 0.1$	$x = 0.5$	α -TeI ₄	β -TeI ₄	TeCl ₄	$\alpha(\beta)$ -TeI
CN(Te)	4.2 ± 1.3	4.0 ± 1.3	6	6	6	3.5 ± 0.5
CN(Te–Te)	0.7 ± 0.7	0.6 ± 0.8	0	0	0	2.0
CN(Te–Cl)	3.3 ± 1.2	2.6 ± 1.2	0	0	6	0
CN(Te–I)	0.2 ± 0.4	0.8 ± 0.8	6	6	0	1.5 ± 0.5
CN(Cl–Te)	1.7 ± 0.8	1.7 ± 0.7	0	0	1.5 ± 0.9	0
CN(I–Te)	1.6 ± 0.6	1.5 ± 0.7	1.6 ± 0.8	1.5 ± 0.7	0	1.5 ± 0.5

of the samples very difficult. In the search of more stable solid tellurium(II) halides we found the stabilizing effect of a mixed Cl/I halogen content. The stabilizing effect of small quantities of iodine in TeCl₂ is so pronounced that solids of the composition TeCl_{2-x}I_x with even a small iodine content like $x = 0.1$ are stable at ambient temperature for several days, i.e., sufficiently long to be examined in the glassy state without decomposition into TeCl₄ and elemental Te or crystalline tellurium subhalides. The increasing ability of glass formation with increasing iodine content in TeX₂ can be probably related to (i) the relatively low enthalpy of the Te–I bonds (121 kJ/mol) compared to those of Te–Cl (311 kJ/mol) and Te–Te bonds (259.8 kJ/mol)²⁸ and (ii) the hypothesis of Goodman,²⁹ according to which the glass formation in a given system is enhanced in the presence of several complex crystalline structures in the corresponding compositional range.

Thermal Analyses. The thermal properties of both samples have been analyzed in closed (DSC) and open (DTA/TG) system. The DSC curves show strong exothermic effects with an onset at 142–145 °C and a maximum at 156 °C for TeCl_{1.9}I_{0.1} and 154 °C for TeCl_{1.5}I_{0.5}. These exothermic effects with energies of about 230 kJ mol⁻¹ are attributed to crystallization processes. For TeCl_{1.9}I_{0.1}, a sharp DSC endothermic signal is observed at 185 °C, corresponding to melting (see Figure 2). The DTA curves show also endothermic melting maxima between 170 and 200 °C, which are close to the melting temperatures of TeCl₄ (223 °C)⁷ and TeI (185 °C)⁷ and additional very strong endothermic effects at 340 °C for both compositions. In the TG curves, these effects are accompanied by a mass loss starting at 240 °C and ending at 350 °C. The mass loss amount is 90% for both compositions, thus indicating sublimation processes. Glass transitions, expected in the temperature region around 100 °C,¹⁸ could, however, not be safely identified. To examine the crystalline products formed by thermally induced recrystallization, TeCl_{2-x}I_x glasses with different compositions were annealed in closed ampules for several days at 100 °C. All samples with different iodine content x between 0.1 and 1.0 were completely transformed under these conditions. With application of a temperature gradient, the crystalline products were transported to the colder part of the ampule and could in most cases be identified by single-crystal unit-cell determinations. For all glass compositions crystals of TeCl₄ with colors from light yellow to orange

sublimated off. For $x = 0.5$ black needle-shaped crystals of α -TeI were found, and for $x = 0.1$ dark crystals of Te₃Cl₂ were identified.

Diffraction Results. The reduced structure factors, $F(Q) = Q^*[S(Q) - 1] = Q^*[I_{\text{coh}}(Q)/\langle f^2 \rangle - 1]$, are given in Figure 3. The X-ray data show structural oscillations up to 24 Å⁻¹, which demonstrates the importance of using hard X-rays. A weak prepeak at about 1.625 Å⁻¹, observed as a shoulder, has been interpreted as a manifestation of medium-range order (MRO) in covalently bonded glasses.³⁰

RMC Fits. Besides the experimental X-ray structure factors, Figure 3 shows the simulated RMC reduced structure factors for TeCl_{1.9}I_{0.1} and TeCl_{1.5}I_{0.5}. The models reproduce well all features in the experimental $F(Q)$.

The corresponding total pair correlation functions $g(r)$, calculated with average weighting coefficients, are shown in Figure 4. The RMC simulations reproduce all features of the experimental $g(r)$ functions. Below 1.9 Å the experimental $g(r)$ were corrected for residual systematic errors using the method of Kaplow et al.³¹ The noise in the simulated $g(r)$ is slightly larger compared to that in the simulated $F(Q)$, because the actual fits were made in reciprocal space.

For samples containing three types of atoms (Te, Cl, and I) the total pair correlation functions $g(r)$ in Figure 4 will contain six different partial pair correlation functions (PPCF): Te–Te; Te–Cl; Te–I; Cl–Cl; Cl–I; I–I. A comparison of the Te–I, Te–Cl, and Te–Te PPCF's is made in Figure 5. For clarity, the halogen–halogen PPCF's, being very similar with only one peak at about 3.3–3.6 Å, are not shown in Figure 5. The Te–Te PPCF's (Figure 5a) show structural oscillations up to 18 Å, which might indicate extended Te–Te MRO. On the other hand, the Te–Cl (Figure 5b) and Te–I (Figure 5c) PPCF's show structural oscillations that reach only up to about 8–10 Å. The peaks at about 4.1 and 5.8 Å in the Te–Te, Te–Cl, and Te–I PPCF's are more well expressed in the TeCl_{1.5}I_{0.5} glass, which indicates that the MRO in the TeCl_{1.5}I_{0.5} sample is more pronounced.

In both compositions, the nearest-neighbor Te–Te distance (Te–Te1) is about 2.7 Å and three different nearest-neighbor Te–Cl distances (Te–Cl1) are observed at about 2.38, 2.45, and 2.70 Å. The first Te–Cl distance is close to the Te–Cl distance reported for TeCl₂ in the gas phase (2.34 Å)⁴ and to the shortest Te–Cl distance in TeCl₄ (2.30 Å).¹⁹ For

(28) Kerr, J. A. In *CRC Handbook of Chemistry and Physics: A Ready-Reference Book of Chemical and Physical Data*; Lide, O. R., Ed.; CRC Press: Boca Raton, FL, 2000.

(29) Goodman, G. H. L. *Nature (London)* **1975**, 257, 370.

(30) Elliot, S. R. *Phys. Rev. Lett.* **1991**, 67, 711.

(31) Kaplow, R.; Averbach, B. L.; Strong, S. L. *J. Phys. Chem. Solids* **1964**, 25, 1196.

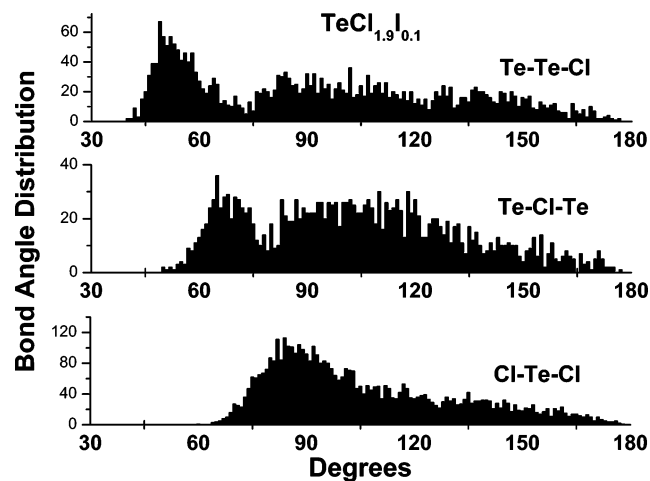


Figure 6. Te–Te–Cl, Te–Cl–Te, and Cl–Te–Cl bond-angle distributions for the $\text{Te}_2\text{Cl}_{1.9}\text{I}_{0.1}$ glass.

$\text{TeCl}_{1.9}\text{I}_{0.1}$, only one nearest-neighbor Te–I (Te–II) distance is observed at about 2.72 Å, while for $\text{TeCl}_{1.5}\text{I}_{0.5}$ there are two peaks at about 2.55 and 2.75 Å (Figure 5c). There is also a tendency that the PPCF peaks of the $\text{TeCl}_{1.5}\text{I}_{0.5}$ glass in the range 2–4.5 Å are broader than those of the $\text{TeCl}_{1.9}\text{I}_{0.1}$ glass, which suggests larger bond-length distortions of the local configurations in $\text{TeCl}_{1.5}\text{I}_{0.5}$.

The Te–Te, Te–Cl, and Te–I nearest neighbors show in both models distributions of coordination numbers. For example, in the $\text{TeCl}_{1.5}\text{I}_{0.5}$ structure 51.8% of the Te atoms are not coordinated by other Te atoms, 35% are coordinated by one Te, 11% are coordinated to two Te atoms, and 2% are coordinated to three Te atoms. Table 1 shows the mean nearest-neighbor coordination numbers, calculated in the range 1.9–3.2 Å, and the half widths of the corresponding coordination distributions, given in parentheses as standard deviations. The coordination of the Te atoms is practically the same in both glasses. Each Te atom is coordinated on average by 3.4 X atoms and 0.7 Te atoms. The number of Te–Cl bonds decreases at the expense of the Te–I bonds, while the number of X–Te bonds remains practically constant (1.7 ± 0.6) with increasing iodine content.

The Te–Te–Cl, Te–Cl–Te, and Cl–Te–Cl bond-angle distributions for the $\text{TeCl}_{1.9}\text{I}_{0.1}$ composition are shown in Figure 6. The bond-angle distributions for the $\text{TeCl}_{1.5}\text{I}_{0.5}$ compositions are similar and are not given for clarity. All bond-angle distributions are very broad as found also in other Te–X¹⁶ and silicate glasses.³² These results suggest the presence of significant bond-angle distortions of the coordination polyhedra. The Te–Te–Cl bond-angle distribution shows a maximum at about 53°, which is not present in the different structure types of tellurium monoiodide α - and β -TeI. The mean Te–Cl–Te bond angles, calculated from the corresponding distributions, are 103.3 and 100.5° for $\text{TeCl}_{1.9}\text{I}_{0.1}$ and $\text{TeCl}_{1.5}\text{I}_{0.5}$, respectively. The Cl–Te–Cl bond-angle distributions have maxima at about 87° and mean values equal to 105.5 and 107.6°, respectively. The latter values are larger than the Cl–Te–Cl bond angle of 98.4°,

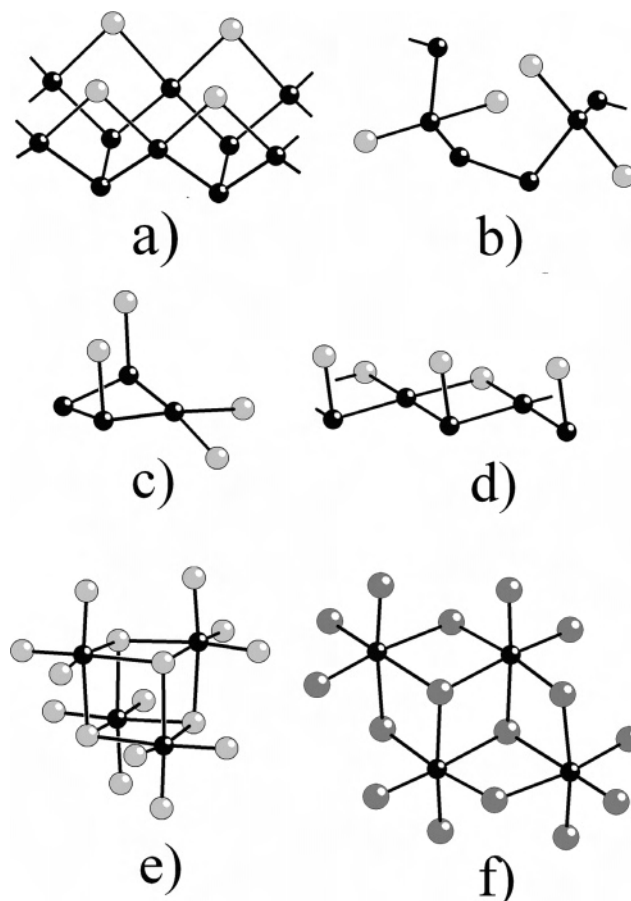


Figure 7. Structure fragments of tellurium iodides and chlorides used for the structural comparison with the $\text{TeCl}_{2-x}\text{I}_x$ glasses: (a) Te_2I_2 ;² (b) Te_3Cl_2 ;² (c) α -TeI;² (d) β -TeI;² (e) TeCl_4 ;¹⁹ ϵ -TeI₄;³³ (f) α -TeI₄.³⁴ Small black spheres are Te atoms, and small and big gray spheres are Cl and I atoms, respectively.

suggested for gaseous TeCl_2 ,⁴ as well as larger than the average X–Te–X bond angles in TeI_4 (101.1°)³³ and TeCl_4 ($94.8 \pm 1.2^\circ$).¹⁹

Discussion

The comparison of the first nearest-neighbor distances in crystalline tellurium halides (Figure 7) shows that both Te and X atoms (X = Cl, I) appear in the first coordination sphere of Te at distances between 2.4 and 3.3 Å. The longest Te–I distance in crystalline Te_2I_2 , for example, is 3.18 Å.² The composition of the investigated amorphous TeX_2 halides is between those of TeX_4 and the subvalent tellurium monoiodide TeI. In the TeX_4 structures (Figure 7e,f), each Te atom is coordinated by 6 halogen atoms at distances ranging from 2.30 Å for TeCl_4 up to 3.32 Å for β -TeI₄.³⁰ The Te–Cl distances in the glassy $\text{TeCl}_{2-x}\text{I}_x$ (2.38–2.70 Å) fall well within this range. The halogen atoms show a more complex environment. In α - and β -TeI₄ as well as in TeCl_4 , there are three crystallographically different halogen atom positions, coordinated by 1, 2, and 3 Te atoms, respectively, while in ϵ -TeI₄ there are only 1 and 3 coordinated I atoms. In the structures of α - and β -TeI, on the other hand, there

(33) Kniep, R.; Beister, H. J.; Wald, D. Z. *Naturforsch.* **1988**, B43, 966.

(34) Krebs, B.; Paulat, V. *Acta Crystallogr.* **1976**, B32, 1470.

(32) Yaung, X. L.; Cormack, A. J. *Non-Cryst. Solids* **2003**, 319, 31.

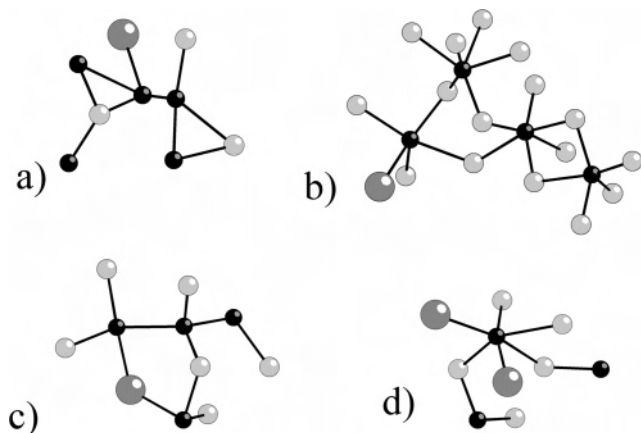


Figure 8. Small clusters (radius ~ 5 Å) extracted from the RMC models: (a, b) $\text{TeCl}_{1.9}\text{I}_{0.1}$; (c, d) $\text{TeCl}_{1.5}\text{I}_{0.5}$. Small black spheres are Te atoms, small light gray spheres are Cl atoms, and big dark gray spheres represent I atoms, respectively.

are two different Te atoms, coordinated by 2 Te + 2 I and 2 Te + 1 I atoms, respectively (see Table 1 and Figure 7c as well as Figure 7d). The iodine atoms in these structures are coordinated either by 1 or 2 Te atoms.

The mean coordination numbers of the halogen atoms in the RMC models (see Table 1) are very similar to the respective average coordination in the crystalline compounds, suggesting similar interconnections of the coordination polyhedra. The average Te–Te and Te–X coordination numbers in the glass models are intermediate between those in crystalline TeX and TeX_4 , suggesting that the structure of the TeX_2 glasses is a mixture of $[\text{TeX}_6]$ building blocks typical for the TeX_4 structures and $\text{Te}[\text{Te}_2\text{X}_2]$ as well as $\text{Te}[\text{Te}_2\text{X}]$ blocks, typical for the TeI structures. Detailed analysis of the models revealed, indeed, the presence of a range of $\text{Te}[\text{Te}_m\text{X}_n]$ clusters, where m and n are the number of Te and halogen atoms in the first coordination sphere of the central Te atom. However, we do not observe extended Te–Te chains as present in Te-rich phases like Te_2I (Figure 7a) or Te_3Cl_2 (Figure 7b). Figure 8a,c shows typical $\text{Te}[\text{Te}_2\text{Cl}_2]$ and $\text{Te}[\text{Te}_2\text{Cl}]$ clusters, which are the building blocks of the TeX structures (see Figure 7c,d). Figure 8b,d shows $\text{Te}[\text{X}_6]$ clusters forming Te_2X_2 rings and chains with Te–Cl–Te angles close to 90° , which are the building blocks of the TeX_4 structures (see Figure 7e,f).

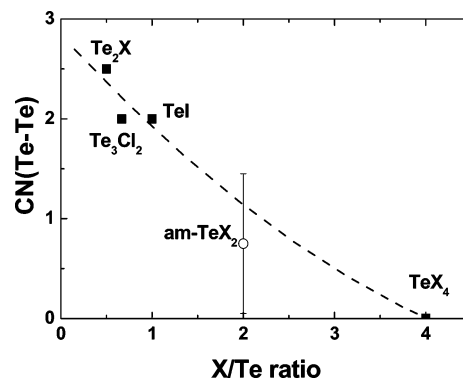


Figure 9. Average coordination of Te atoms directly coordinated by other Te atoms versus X/Te ratio: crystalline Te halides (filled squares); amorphous TeX_2 (empty circle). The dashed line is only a guide for the eye.

The average Te–Te coordination in crystalline halides decreases almost linearly with increasing X/Te ratio (Figure 9). The average Te–Te coordination in the investigated TeX_2 glasses fits this trend within error limits.

Conclusions

The structures of two Te–X glasses with compositions $\text{Te}_2\text{Cl}_{1.9}\text{I}_{0.1}$ and $\text{Te}_2\text{Cl}_{1.5}\text{I}_{0.5}$ have been studied by reverse Monte Carlo (RMC) fits to the corresponding structure factors obtained from high-energy X-ray diffraction measurements. The TeX_2 glasses consist of structural building blocks characteristic for both the TeI and TeX_4 ($X = \text{Cl}, \text{I}$) crystalline phases. The coordination polyhedra of the Te atoms are generally strongly distorted. A decrease of the average Te–Te coordination in crystalline and amorphous Te halides with increasing X/Te ratio is established. To gain further insight in the structure it would be interesting to perform neutron diffraction experiments on ^{37}Cl -enriched TeX_2 samples to determine the Cl–Cl and Cl–Te partial pair correlation functions more reliably.

Acknowledgment. This work has been supported by the Deutsche Forschungsgemeinschaft (German Research Council) within the Sonderforschungsbereich 408 (Collaborative Research Area 408). We thank Dr. P. Jovari for the help in performing the X-ray diffraction experiments as well as Dr. J. Daniels and V. Bendisch for the single-crystal work.

IC062307Q